Electronic Supplementary Material (ESI) for Journal of Materials Chemistry A.

SiO_2 assisted Cu^0-Cu^+-NH_2 composite interfaces for efficient CO_2 electroreduction to C_{2+} products

Zi-Yang Zhang,‡[a] Hao Tian,‡[a] Han Jiao,[a] Xin Wang,[a] Lei Bian,[a] Yuan Liu,[a]

Nithima Khaorapapong,[b] Yusuke Yamauchi,[c,d,e] and Zhong-Li Wang[a,*]

[a] Tianjin Key Laboratory of Applied Catalysis Science & Technology, School of Chemical Engineering and Technology, Tianjin University, Tianjin 300072, China
*Email: wang.zhongli@tju.edu.cn

[b] Materials Chemistry Research Center, Department of Chemistry and Center of Excellence for Innovation in Chemistry, Faculty of Science, Khon Kaen University, Khon Kaen 40002, Thailand

[c] Australian Institute for Bioengineering and Nanotechnology (AIBN), The University of Queensland, Brisbane, QLD 4072, Australia

[d] Department of Materials Process Engineering, Graduate School of Engineering, Nagoya University, Nagoya, 464−8603 Japan

[e] Department of Chemical and Biomolecular Engineering, Yonsei University, 50 Yonsei-ro, Seodaemun-gu, Seoul, 03722 South Korea

‡ The authors contributed equally to this work.

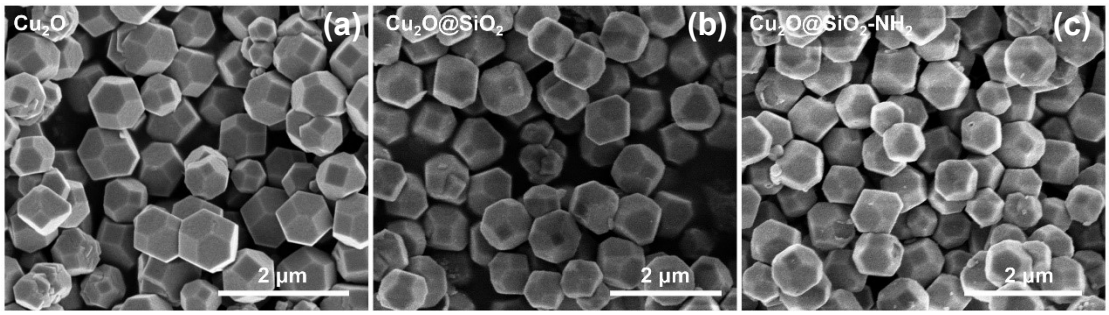

Fig. S1 The SEM images of (a) Cu_2O, (b) $Cu_2O@SiO_2$ and (c) $Cu_2O@SiO_2$-NH_2 catalysts.

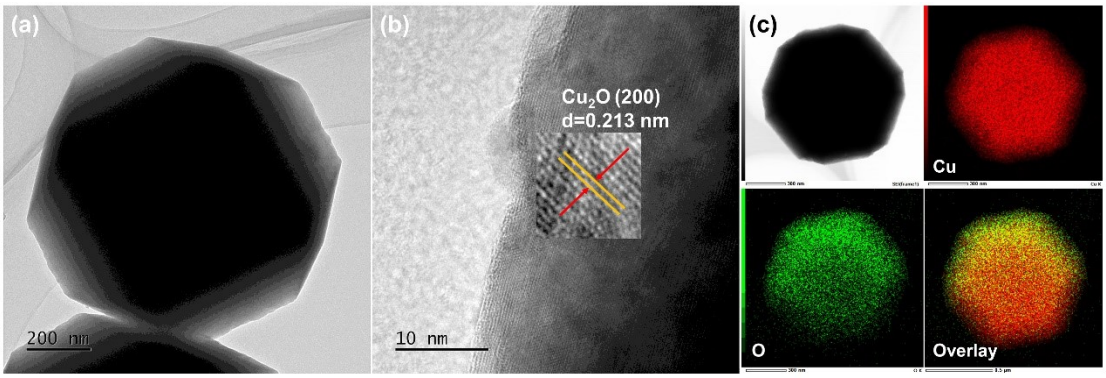

Fig. S2 Morphological and structural characterizations of Cu_2O. (a) TEM image; (b) HR-TEM image and (c) EDX mapping.

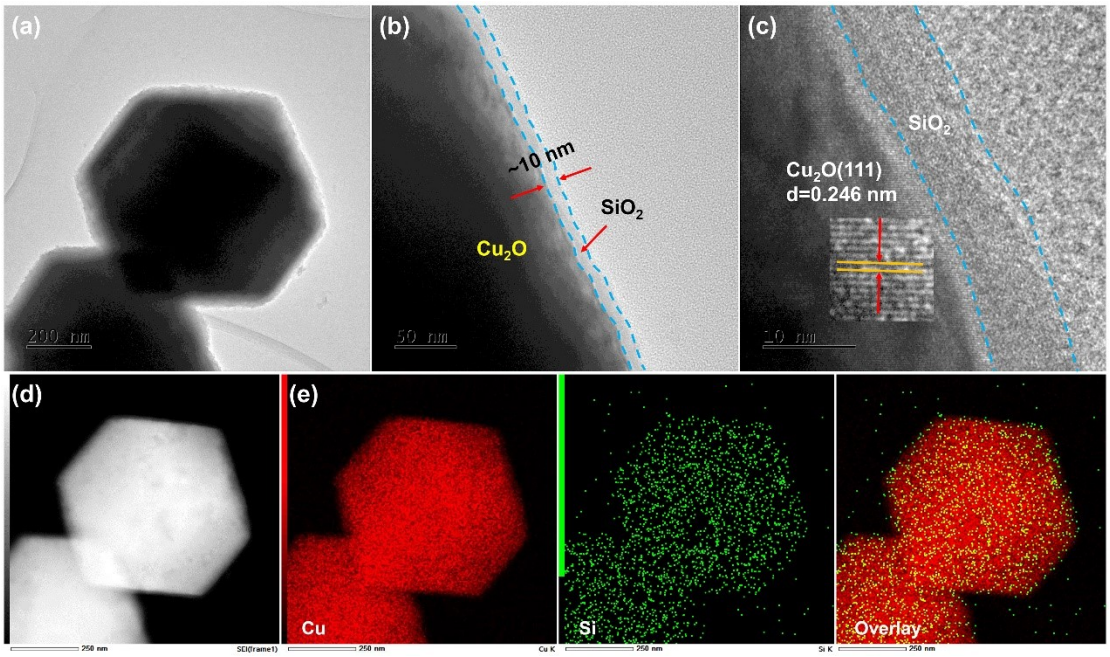

Fig. S3 Morphological and structural characterizations of $Cu_2O@SiO_2$. (a, b) TEM images; (c) HR-TEM image; (d) HAADF-STEM image and (e) EDX mapping.

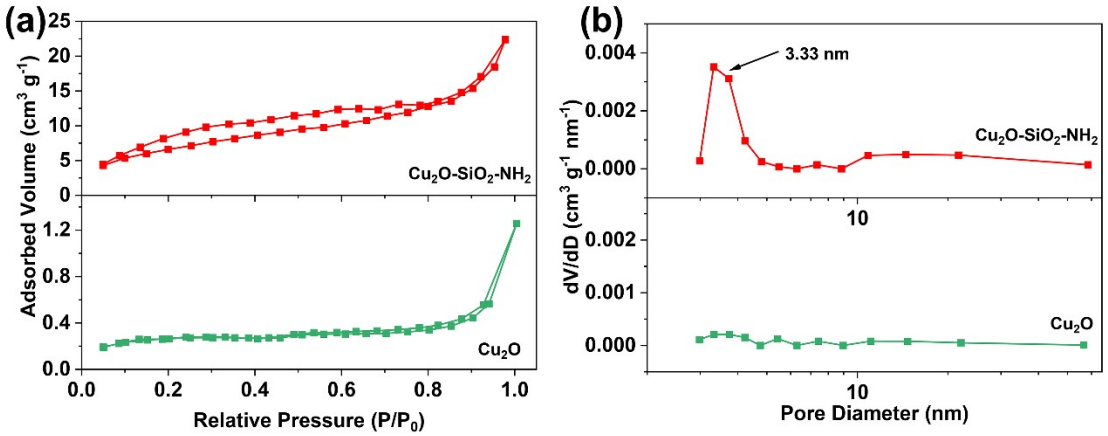

Fig. S4. (a) N_2 adsorption-desorption isotherms and (b) The pore size distribution curves of Cu_2O and Cu_2O@SiO_2-NH_2 catalysts.

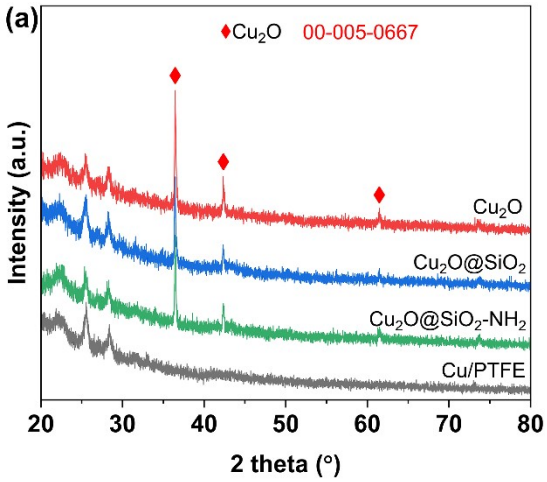

Fig. S5 XRD patterns of Cu_2O, $Cu_2O@SiO_2$ and $Cu_2O@SiO_2$-NH_2 catalysts on the Cu/PTFE substrate.

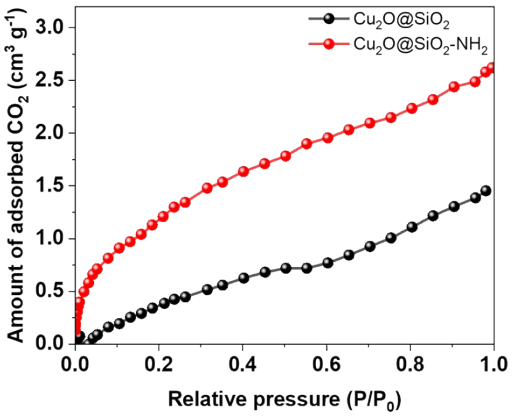

Fig. S6 The CO_2 adsorption isotherms of $Cu_2O@SiO_2$-NH_2 and $Cu_2O@SiO_2$.

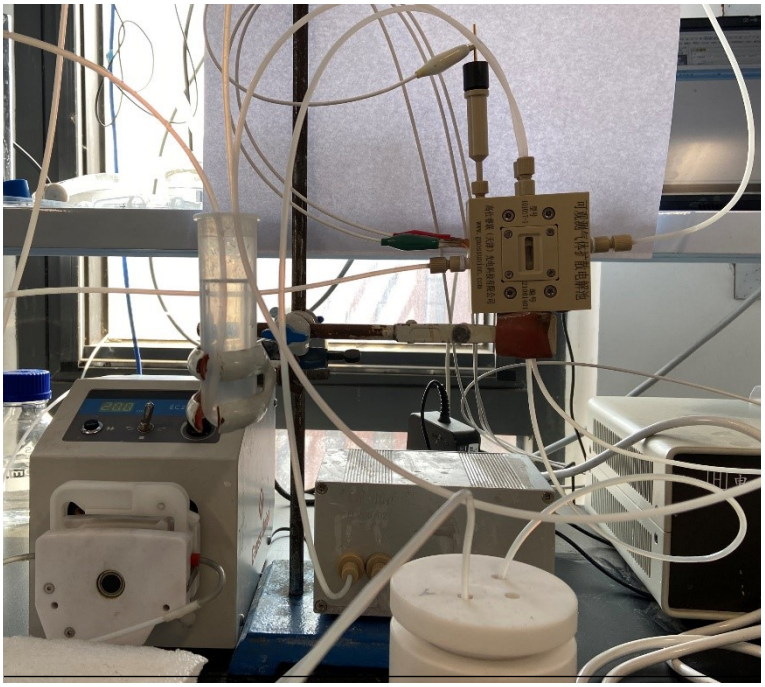

Fig. S7 Electrochemical CO_2 reduction reaction system.

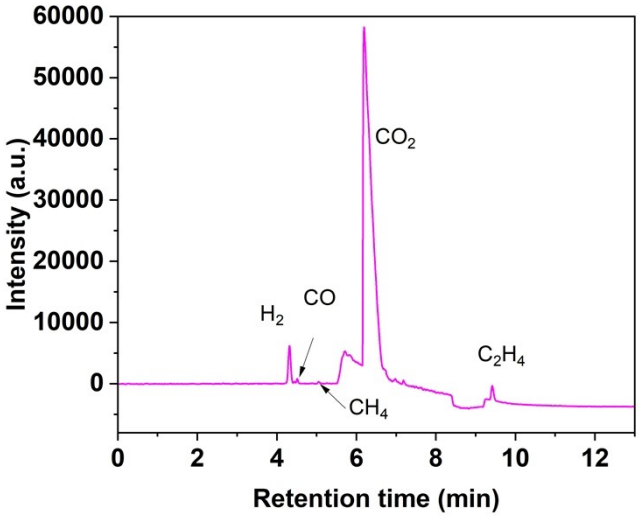

Fig. S8 Gas chromatography for gas products in CO_2RR on the $Cu_2O@SiO_2$-NH_2 catalyst at the current density of 280 mA cm^{-2}.

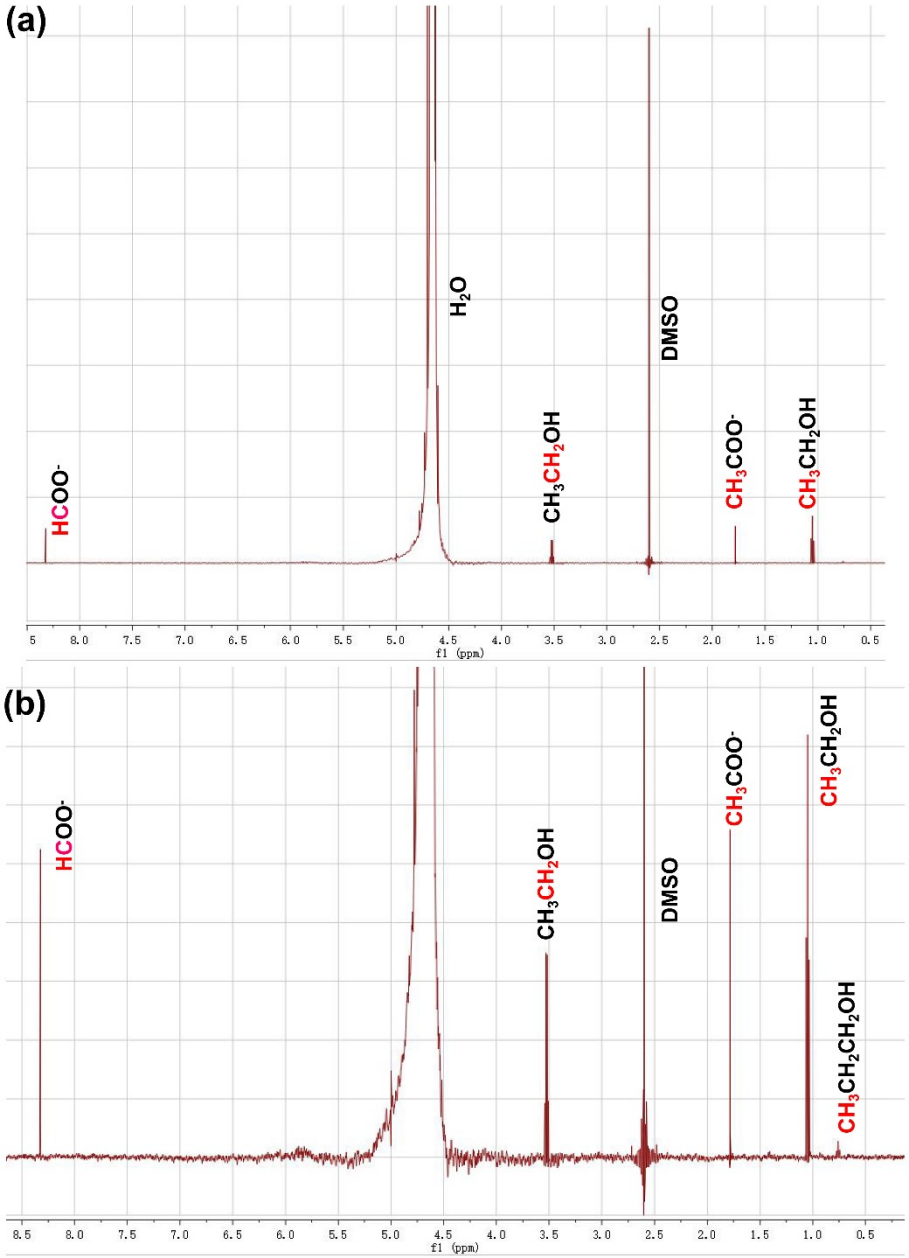

Fig. S9 (a) ^{1}H NMR spectrum for liquid phase products in CO_2RR on Cu_2O@SiO_2-NH_2 catalyst at the current density of 280 mA cm^{-2}. (b) is an enlarged view of (a). DMSO is used as internal standard.

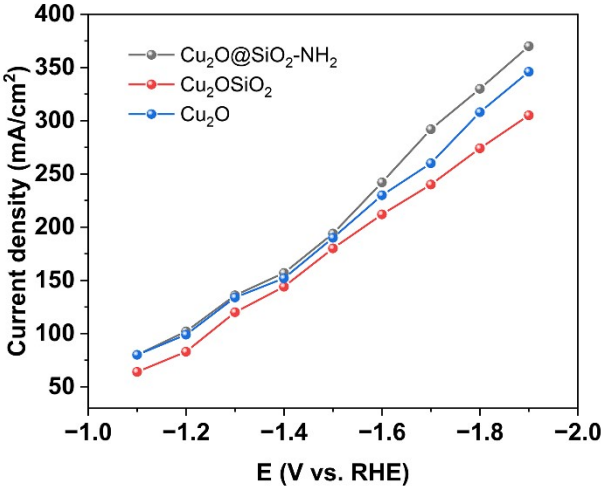

Fig. S10 The current densities of CO_2RR on $Cu_2O@SiO_2$-NH_2, $Cu_2O@SiO_2$ and Cu_2O catalysts.

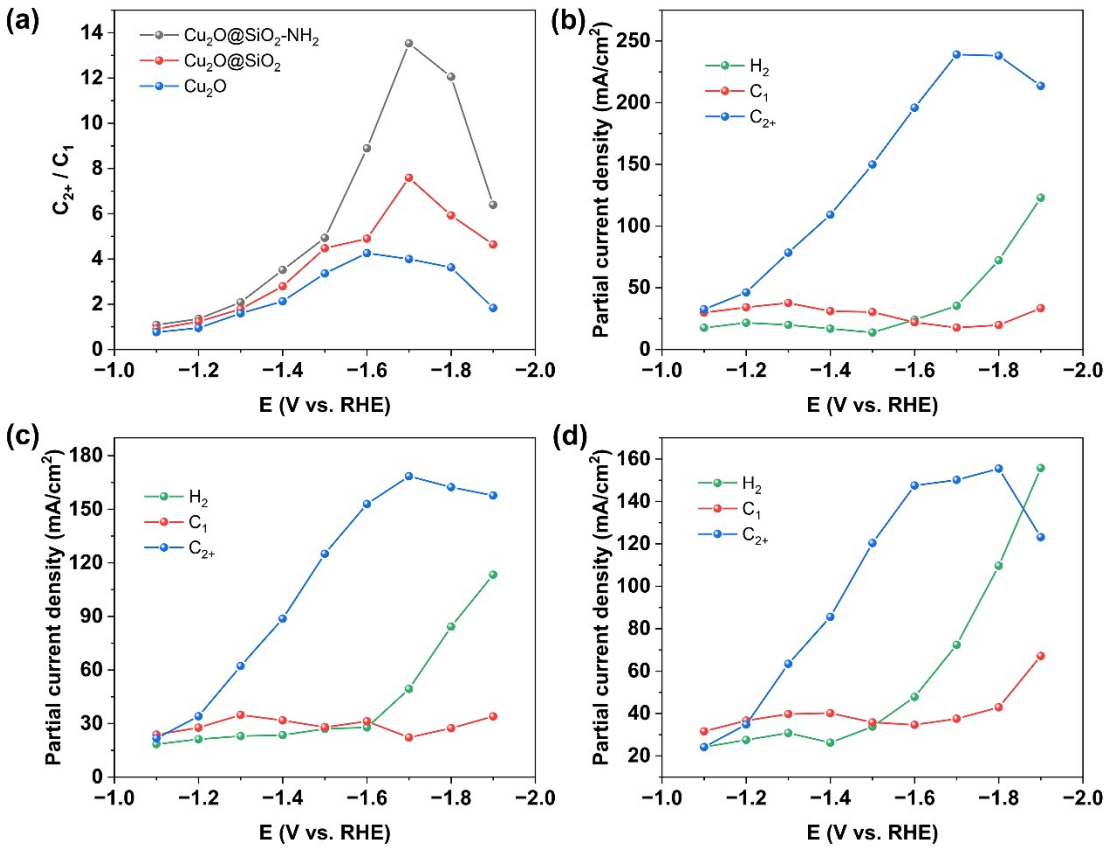

Fig. S11 (a) The ratios of C_{2+}/C_1 products and the partial current densities of products in CO_2RR on (b) $Cu_2O@SiO_2$-NH_2, (c) $Cu_2O@SiO_2$ and (d) Cu_2O catalysts.

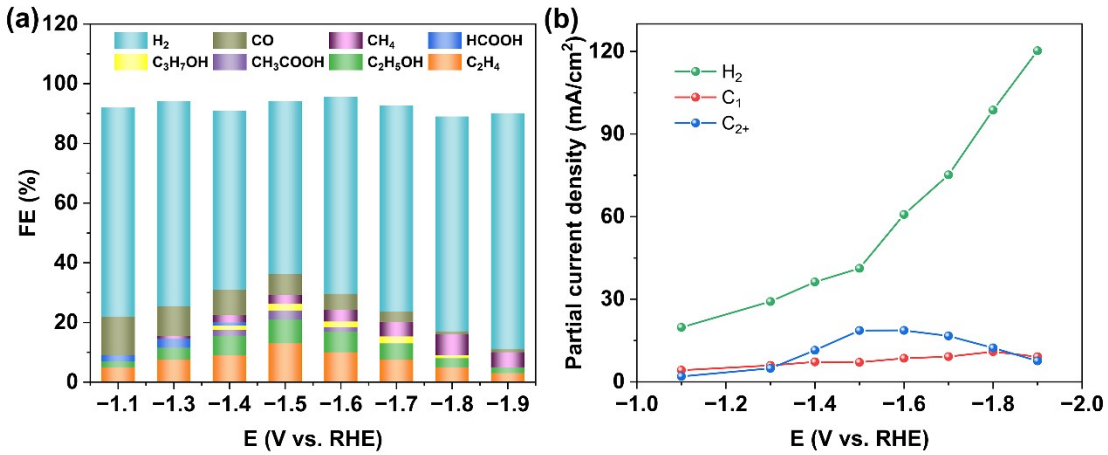

Fig. S12 The product distributions and partial current densities of CO_2RR over the Cu/PTFE substrate. (a) Product distributions and (b) Partial current densities.

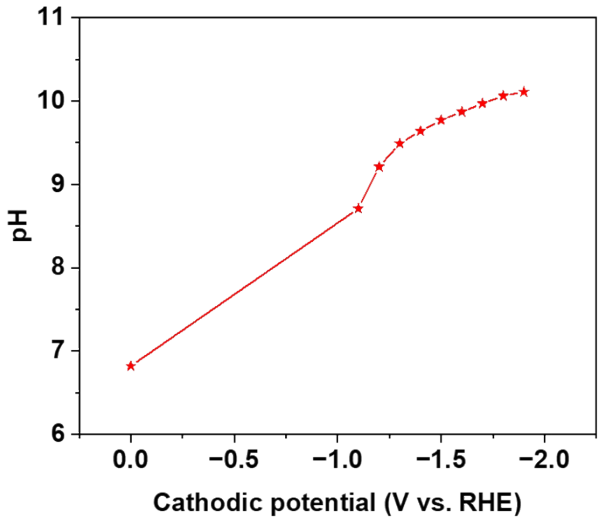

Fig. S13 The pH values of the electrolyte during CO_2RR.

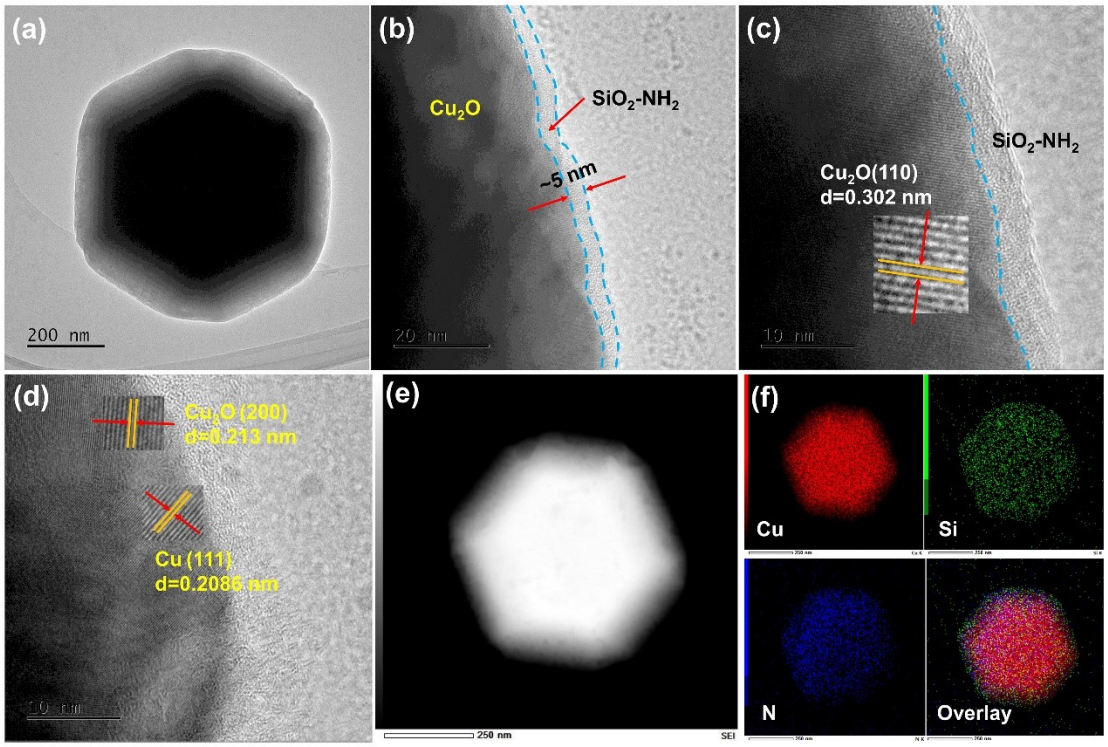

Fig. S14 Morphological and structural characterizations of Cu_2O@SiO_2-NH_2 after the CO_2RR test. (a and b) TEM images; (c and d) HR-TEM images; (e) HAADF-STEM image and (f) EDX mapping.

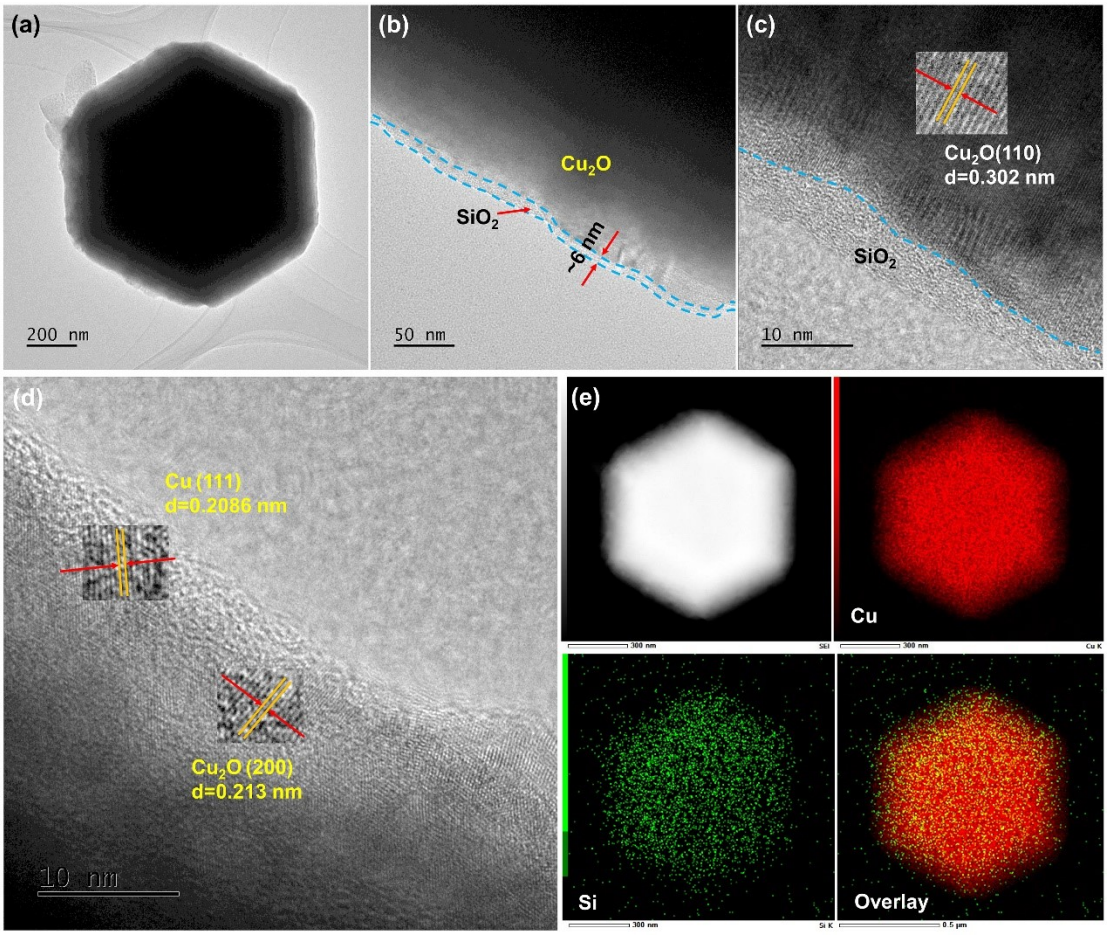

Fig. S15 Morphological and structural characterizations of Cu_2O@SiO_2 after the CO_2RR test. (a and b) TEM images; (c and d) HR-TEM images; (e) EDX mapping.

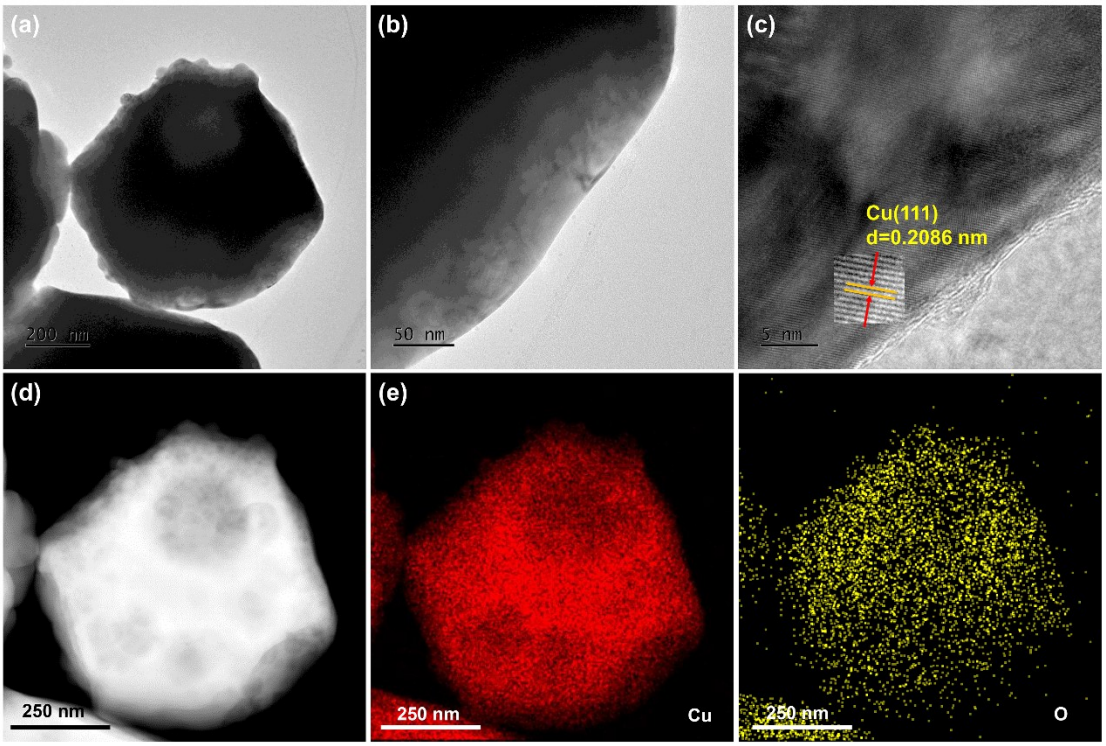

Fig. S16 Morphological and structural characterizations of Cu_2O after the CO_2RR test. (a and b) TEM images; (c) HR-TEM image; (d) HAADF-STEM image and (e) EDX mapping.

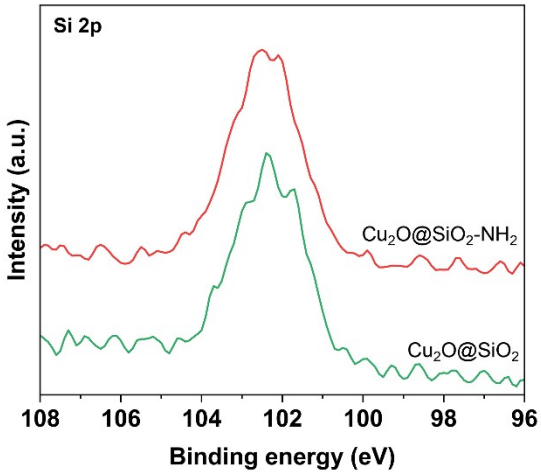

Fig. S17 Si 2p XPS spectra of $Cu_2O@SiO_2$ and $Cu_2O@SiO_2$-NH_2 catalysts after the CO_2RR test.

Table S1. Comparison of the FE of C_{2+} and the partial current density of C_{2+} with other electrocatalysts reported previously.

Catalyst	FE of C_{2+}	C_{2+} partial current density (mA/cm^2)	Electrolyte	Electrolyzer	Publication Time	Ref.
Cu_3N	73.7	810	1 M KOH	Flow cell	2022	1
Mg-Cu alloy	80	800	1 M KOH	Flow cell	2022	2
$Cu_2O/Ag_{2.3\%}$	82.1	656.8	1 M KOH	Flow cell	2022	3
K-F-Cu-CO_2	77	616	1 M KOH	Flow cell	2022	4
Fragmented Cu	77.8	233	7 M KOH	Flow cell	2022	5
$Cu_2P_2O_7$	73.6	257	/	MEA	2022	6
CuO nanoplate arrays	85.4	93.5	0.5 M KCl	Flow cell	2022	7
Cu_2O superparticle-CP3	74.2	30	0.1 M $KHCO_3$	H-cell	2022	8
CuO-nr/CC3	76.1	1293	1 M KOH	Flow cell	2022	9
BiCu-SAA	72.6	290	1 M KOH	Flow cell	2023	10
Cu-12C	86.1	103.3	1 M KOH	Flow cell	2023	11
M-Cu_1/Cu_{NP}	75.4	289.2	5 M KOH	Flow cell	2023	12
25 nm Cu-coated GDE	73	110	6.33 M $NaClO_4$	Flow cell	2023	13
EC-Cu-2	90	180	0.05M H_2SO_4+2.5M	Flow cell	2023	14

			KCl			
Dual-phase copper	81	322	3 M KCl	Flow-cell	2023	15
$Cu_2O@SiO_2$-NH_2	**81.7**	**237**	**1 M KCl**	**Follow cell**		**This work**

Table S2. Cathode CO_2RR equations.

CO_2 reduction reaction
$x\,CO_2 + n\,H^+ + n\,e^- \rightarrow products + y\,H_2O$
$CO_2 + 2H^+ + 2e^- \rightarrow HCOOH_{(aq)}$
$CO_2 + 2H^+ + 2e^- \rightarrow CO_{(g)} + H_2O$
$CO_2 + 6H^+ + 6e^- \rightarrow CH_3OH_{(aq)} + H_2O$
$CO_2 + 8H^+ + 8e^- \rightarrow CH_{4(g)} + 2H_2O$
$2CO_2 + 8H^+ + 8e^- \rightarrow CH_3COOH_{(aq)} + 2H_2O$
$2CO_2 + 10H^+ + 10e^- \rightarrow CH_3CHO_{(aq)} + 3H_2O$
$2CO_2 + 12H^+ + 12e^- \rightarrow C_2H_5OH_{(aq)} + 3H_2O$
$2CO_2 + 12H^+ + 12e^- \rightarrow C_2H_{4(g)} + 4H_2O$
$2CO_2 + 14H^+ + 14e^- \rightarrow C_2H_{6(g)} + 4H_2O$
$3CO_2 + 16H^+ + 16e^- \rightarrow C_2H_5CHO_{(aq)} + 5H_2O$
$3CO_2 + 18H^+ + 18e^- \rightarrow C_3H_7OH_{(aq)} + 5H_2O$

Reference:

1 M. Zheng, P. Wang, X. Zhi, K. Yang, Y. Jiao, J. Duan, Y. Zheng, S. Z. Qiao, J. Am. Chem. Soc., 2022, **144**, 14936-14944.

2 M. Xie, Y. Shen, W. Ma, D. Wei, B. Zhang, Z. Wang, Y. Wang, Q. Zhang, S. Xie, C. Wang, Y. Wang, Angew. Chem. Int. Ed., 2022, **61**, e202213423.

3 P. Wang, H. Yang, C. Tang, Y. Wu, Y. Zheng, T. Cheng, K. Davey, X. Huang, S. Z. Qiao,Nat. Commun., 2022, **13**, 3754.

4 C. Peng, S. Yang, G. Luo, S. Yan, M. Shakouri, J. Zhang, Y. Chen, W. Li, Z. Wang, T. K. Sham, G. Zheng, Adv. Mater., 2022, **34**, 2204476.

5 K. Yao, J. Li, H. Wang, R. Lu, X. Yang, M. Luo, N. Wang, Z. Wang, C. Liu, T. Jing, S. Chen, E. Cortes, S. A. Maier, S. Zhang, T. Li, Y. Yu, Y. Liu, X. Kang, H. Liang, J. Am. Chem. Soc., 2022, **144**, 14005-14011.

6 J. Sang, P. Wei, T. Liu, H. Lv, X. Ni, D. Gao, J. Zhang, H. Li, Y. Zang, F. Yang, Z. Liu, G. Wang, X. Bao, Angew. Chem. Int. Ed., 2022, **134**, e202114238.

7 W. Liu, P. Zhai, A. Li, B. Wei, K. Si, Y. Wei, X. Wang, G. Zhu, Q. Chen, X. Gu, R. Zhang, W. Zhou, Y. Gong, Nat. Commun., 2022, **13**, 1877.

8 Y. Jiang, X. Wang, D. Duan, C. He, J. Ma, W. Zhang, H. Liu, R. Long, Z. Li, T. Kong, X. J. Loh, L. Song, E. Ye, Y. Xiong, Adv. Sci., 2022, **9**, 2105292.

9 C. Chen, X. Yan, Y. Wu, S. Liu, X. Zhang, X. Sun, Q. Zhu, H. Wu, B. Han, Angew. Chem. Int. Ed., 2022, **61**, e202202607.

10 Y. Cao, S. Chen, S. Bo, W. Fan, J. Li, C. Jia, Z. Zhou, Q. Liu, L. Zheng, F. Zhang, Angew. Chem. Int. Ed., 2023, **62**, e202303048.

11 Y. Lin, T. Wang, L. Zhang, G. Zhang, L. Li, Q. Chang, Z. Pang, H. Gao, K. Huang, P. Zhang, Z. Zhao, C. Pei, J. Gong, Nat. Commun., 2023, **14**, 3575.

12 J. Feng, L. Zhang, S. Liu, L. Xu, X. Ma, X. Tan, L. Wu, Q. Qian, T. Wu, J. Zhang, X. Sun, B. Han, Nat. Commun., 2023, **14**, 4615.

13 H. Zhang, J. Gao, D. Raciti, A. S. Hall, Nat. Catal., 2023, **6**, 807–817.

14 Y. Cao, Z. Chen, P. Li, A. Ozden, P. Ou, W. Ni, J. Abed, E. Shirzadi, J. Zhang, D. Sinton, J. Ge, E. H. Sargent, Nat. Commun., 2023. **14**, 2387.

15 P.-P. Yang, X.-L. Zhang, P. Liu, D. J. Kelly, Z.-Z. Niu, Y. Kong, L. Shi, Y.-R. Zheng, M.-H. Fan, H.-J. Wang, M.-R. Gao, J. Am. Chem. Soc., 2023, **145**, 8714–8725.